

hep-ph/9607292
CERN-TH/96-102
CERN-PPE/96-84
UMN-TH-1501/96
TPI-MINN-96/09

Supersymmetric Dark Matter in the Light of LEP 1.5

John Ellis¹, Toby Falk,² Keith A. Olive,² and Michael Schmitt³

¹*TH Division, CERN, Geneva, Switzerland*

²*School of Physics and Astronomy, University of Minnesota, Minneapolis, MN 55455, USA*

³*PPE Division, CERN, Geneva, Switzerland*

Abstract

We discuss the lower limit on the mass of the neutralino χ that can be obtained by combining data from e^+e^- annihilation at LEP and elsewhere with astrophysical and theoretical considerations. Loopholes in the purely experimental analysis of ALEPH data from the Z^0 peak and LEP 1.5, which appear when $\mu < 0$ for certain values of the sneutrino mass $m_{\tilde{\nu}}$ and the ratio $\tan\beta$ of supersymmetric Higgs vacuum expectation values, may be largely or totally excluded by data from lower-energy e^+e^- data, the hypothesis that most of the cosmological dark matter consists of χ particles, and the assumption that electroweak symmetry breaking is triggered by radiative corrections due to a heavy top quark. The combination of these inputs imposes $m_\chi \geq 21.4$ GeV, if soft supersymmetry-breaking masses are assumed to be universal at the grand-unification scale.

CERN-TH/96-102

July 1996

1 Introduction

The recent run of LEP at energies between 130 and 140 GeV, hereafter referred to as LEP 1.5, has provided important new experimental constraints on the spectrum of supersymmetric particles [1, 2, 3, 4]. These include direct lower limits on the masses of the chargino χ^\pm and the right-handed selectron \tilde{e}_R , under certain assumptions on the masses of other sparticles, such as the lightest neutralino χ and the sneutrino $\tilde{\nu}$. Within the context of the Minimal Supersymmetric extension of the Standard Model (MSSM) [5], these direct limits from LEP 1.5 have been combined by ALEPH with previous limits on sparticle production at LEP 1 to obtain indirect lower limits on the neutralino mass m_χ [6], which depend in particular on the assumed value of $m_{\tilde{\nu}}$. Indeed, there are domains of $\tan\beta$ and $m_{\tilde{\nu}}$ in which m_χ could still vanish, in principle [6].

Lower limits on m_χ are potentially of great interest to experimental searches for supersymmetric dark matter, which is assumed to consist of neutralinos χ [7]. Some experiments are optimized to look for relatively light neutralinos [8], and the prospective recoil energy spectrum close to threshold is of concern to all searches [9]. For these reasons, it is useful to review the ALEPH lower limit on m_χ [6], and to combine it with other phenomenological, cosmological and model considerations, in order to evade the assumptions made in the ALEPH analysis, and/or to strengthen the lower limit in the presence of additional assumptions.

Cosmological arguments complementing ALEPH's purely experimental analysis are the primary focus of this paper, whose outline is as follows. After a brief review of the ALEPH lower limit on m_χ [6], in which we flag aspects in which this experimental analysis may be supplemented, we first refine some relevant phenomenological considerations. In addition to the lower limit on $m_{\tilde{\nu}}$ from invisible Z^0 decays, and the absence of sleptons at LEP 1.5 [1, 3], these include the interpretation of searches at PEP and TRISTAN for single-photon events [10], which plays an important rôle in excluding a massless neutralino in a particular domain of $\tan\beta$ and $m_{\tilde{\nu}}$ ¹. However, these experiments do not exclude the possibility that $m_{\tilde{\nu}}$ is slightly less than m_{χ^\pm} , in which case the available lower limits on m_{χ^\pm} are weakened [1, 2, 3, 4], and the lower limit [6] on m_χ requires further discussion². For this purpose, we introduce the cosmological considerations which are our primary interest. These include the requirement that relic neutralinos [7] not be overdense: $\Omega_\chi h^2 \leq 0.3$, and also the preference

¹As in [6], we assume universality of the gaugino masses: $M_{i=1,2,3} = m_{1/2}$ at the grand-unification scale, and also universality of the soft supersymmetry-breaking scalar masses: $m_{\tilde{\nu}} = m_{\tilde{e}} = m_0$.

²We focus in this paper on the case in which the Higgs superpotential mixing parameter $\mu < 0$, since this is when loopholes in the ALEPH analysis [6] allow $m_\chi = 0$. We also make a few remarks on the case $\mu > 0$, deferring a more complete analysis of this case to a later paper.

that they have sufficient density to be of astrophysical interest: $\Omega_\chi h^2 \geq 0.1$, where h is the current Hubble expansion rate, in units of 100 km/s/Mpc. Finally, we supplement these phenomenological constraints with the theoretical Ansatz of electroweak symmetry breaking driven dynamically by radiative corrections associated with a heavy top quark [11], which reduces the number of supersymmetric model parameters, enabling the lower bound on m_χ to be further strengthened.

In the case of $\mu < 0$ shown in Fig. 1, we find that the e^+e^- annihilation results alone, including the AMY analysis, enforce $m_\chi \gtrsim 5$ GeV, with this limit being reached at $\tan\beta = 2$, and cut off most of the region of low m_χ favored by cosmology. Combining the cosmological constraint with the theoretical assumption of radiative electroweak symmetry breaking strengthens significantly the lower limit on m_χ to 21.4 GeV, which is reached at $\tan\beta \simeq 1.6$, with the lower bound rising above 51 GeV for $\tan\beta \gtrsim 5$. Our bounds for $\tan\beta \gtrsim 2.5$ are stronger than those that can be obtained indirectly from constraints on the Higgs mass [6] in the context of the MSSM with radiative electroweak symmetry breaking. In the case of $\mu > 0$ (not shown), we find for large $m_{\tilde{\nu}}$ that $m_\chi \gtrsim 56$ GeV for $\tan\beta \gtrsim 3$, which is relaxed to $m_\chi \gtrsim 36$ GeV for $\tan\beta \lesssim 3$.

2 Review of Accelerator Constraints

We first review the LEP lower limit on m_χ presented by the ALEPH Collaboration [6], shown for $\mu < 0$ as the dashed line in Fig. 1. This results from the combination of three distinct analyses, corresponding to lines shown in Fig. 2: (A) the search for chargino pair production at LEP 1.5, yielding $m_{\chi^\pm} \gtrsim 67.8$ GeV when $m_{\tilde{\nu}}$ is large, (B) the search for all channels of associated neutralino pair production at LEP 1.5, and (C) the search for $\chi\chi'$ production on the Z^0 peak at LEP 1 [12]. The latter is useful at low $\tan\beta$ when $\mu < 0$, as the high Z^0 statistics enable the exclusion (C) of a wedge of the (M_2, μ) plane between the regions (A,B) ruled out by LEP 1.5, as shown by the arrows in Figs. 2(a,b).

Of particular interest to us are two loopholes in the ALEPH analysis [6] that appear when $\mu < 0$. One is that the lower bound on m_{χ^\pm} is relaxed for smaller values of $m_{\tilde{\nu}}$, so that the LEP 1.5 and LEP 1 constraints no longer interlock so effectively, opening up the possibility that $M_2 = 0$ for some values of $\mu < 0$ and $\tan\beta$ near $\sqrt{2}$: this is indicated by the double arrow at the bottom of Fig. 1. The other loophole is present only at large $m_{\tilde{\nu}}$, and only for $1 < \tan\beta < 1.02$. The first of these loopholes arises because the lower limit on m_{χ^\pm} is reduced by up to 4 GeV as $m_{\tilde{\nu}}$ is reduced towards m_{χ^\pm} from above, and then disappears entirely for $m_{\chi^\pm} > m_{\tilde{\nu}} \gtrsim m_{\chi^\pm} - 3$ GeV, in which case χ^\pm decay is dominated by $\tilde{\nu} + \text{soft}$

lepton final states. Bounds on chargino production reappear when $m_{\chi^\pm} - m_{\tilde{\nu}} \gtrsim 3$ GeV and the lepton detection efficiency picks up again. The second loophole is a very small allowed region that opens up for $\tan\beta < 1.02$ at small $M_2 \lesssim 5$ GeV and small negative $\mu \simeq -30$ GeV. We note that, although $M_2 = 0$ is allowed in both these loopholes, and the possibility that $\mu = 0$ could not previously be excluded by LEP 1 data alone, the latter possibility has now been excluded by the neutralino searches at LEP 1.5.

The ALEPH lower bound on m_χ based on the three types of searches (A)-(C) mentioned above is translated into the $(m_{1/2}, m_0)$ plane in Fig. 3(a,b,c,d), as the long-dashed lines (marked ‘ALEPH’). We recall that, if gaugino mass universality is assumed,

$$M_2 \simeq 0.82 m_{1/2} \tag{1}$$

and that, in the limit of large $|\mu|$,

$$m_\chi \simeq 0.43 m_{1/2} \tag{2}$$

In computing the long-dashed lines in Fig. 3, the lower limit on m_χ is obtained by varying μ over its allowed range. We see clearly the first and more important of the two loopholes mentioned above, where the long-dashed line in Fig. 3 recedes to the vertical axis. The second and less important loophole has been ignored in drawing the long-dashed line in Fig. 3(a). One of the key issues in our analysis will be the extent to which the two loopholes mentioned above may be plugged by other considerations, such as the other phenomenological constraints which we discuss next, or the cosmological and theoretical considerations which we introduce later.

An important phenomenological constraint is the lower bound on $m_{\tilde{\nu}}$ that may be inferred from the upper limit on Z^0 decays into $\tilde{\nu} \bar{\tilde{\nu}}$ imposed by the LEP 1 determination of the invisible Z^0 decay width, parametrized in terms of the equivalent number of light neutrino species, N_ν . This is quoted by the Particle Data Group [13] as yielding $m_{\tilde{\nu}} > 41.8$ GeV, assuming three degenerate sneutrino species. However, this may be improved by using the latest analysis of the Z^0 lineshape by the LEP Electroweak Working Group [14], which yields $N_\nu = 2.991 \pm 0.016$ corresponding to

$$m_{\tilde{\nu}} > 43.1 \text{ GeV} \tag{3}$$

at the 95 % confidence level. However, even this updated upper bound still allows $m_{\tilde{\nu}}$ into the ‘dangerous’ region where $m_{\tilde{\nu}} \lesssim m_{\chi^\pm}$ and the LEP 1.5 chargino search may lose sensitivity, so we also examine other phenomenological constraints. For purposes of comparison, we can

express the constraint (3) in terms of the MSSM parameters m_0 and $m_{1/2}$, using the standard relation

$$m_{\tilde{\nu}}^2 = m_0^2 + 0.52m_{1/2}^2 - 0.50M_Z^2 |\cos(2\beta)| \quad (4)$$

shown as the short-dashed lines in Fig. 3 (marked ‘ $\tilde{\nu}$ ’).

The ALEPH and L3 Collaborations have also published [1, 3] lower bounds on the \tilde{e}_R mass, which extend beyond the limits previously established at LEP 1 by an amount that depends on the χ mass assumed. These may be combined to give a more stringent upper limit on the cross section for acoplanar lepton pairs. Within the MSSM, the different slepton flavours are almost degenerate: $m_{\tilde{e}} \simeq m_{\tilde{\mu}} \simeq m_{\tilde{\tau}} = m_{\tilde{\ell}}$, except possibly at large $\tan\beta$, and there is a specific relation between the ℓ_R and ℓ_L masses:

$$\begin{aligned} m_{\tilde{e}_L}^2 &= m_0^2 + 0.52m_{1/2}^2 - 0.27M_Z^2 |\cos(2\beta)| \\ m_{\tilde{e}_R}^2 &= m_0^2 + 0.15m_{1/2}^2 - 0.23M_Z^2 |\cos(2\beta)| \end{aligned} \quad (5)$$

Therefore, the limits on different slepton flavours in different experiments may easily be combined, and translated into the $(m_{1/2}, m_0)$ plane, as shown in Fig. 3 by the solid lines (marked ‘ $\tilde{\ell}$ ’). For lower values of $\tan\beta$, this combined slepton constraint improves on the $\tilde{\nu}$ mass limit in the $m_{1/2}$ range of interest, but still does not exclude χ^\pm decays into $\tilde{\nu}$ + soft lepton.

Next we consider the constraints imposed by a series of experiments looking for single photons in e^+e^- annihilation, interpreted as γ bremsstrahlung accompanying otherwise invisible $\nu\bar{\nu}$ or $\chi\chi$ final states [15, 16, 17]. Experiments of this type below the Z^0 peak impose significant constraints on $(m_\chi, m_{\tilde{e}})$ that may also be mapped into the $(m_{1/2}, m_0)$ plane. The AMY Collaboration has recently presented their results for the single-photon search, and combined them with previous measurements to exclude domains of $m_{\tilde{\gamma}}$ and $m_{\tilde{e}_L} = m_{\tilde{e}_R}$ [10]. We have converted the AMY analysis into a constraint in the $(m_{1/2}, m_0)$ plane by using the correct general gaugino content of χ to evaluate its couplings to $\tilde{e}_{L,R}$, for which we use the mass relations (5). We use the approximate kinematical formulae of [16] to adjust the AMY mass limit to take account of the difference between the hypothetical couplings of the $\tilde{\gamma}$ and the true couplings of the χ . We show in Fig. 3 this reinterpretation of the AMY analysis within the MSSM. We see that this constraint excludes the possibility that $m_{1/2} = 0$, although it does not exclude all of the region $m_{\chi^\pm} > m_{\tilde{\nu}}$ not excluded by ALEPH. The corresponding AMY lower limit on m_χ appears as the portion of the dotted line in Fig. 1 in the region $1 \leq \tan\beta \leq 2$, excluding $m_\chi = 0$ in the previous loophole region indicated by the double arrow.

The small loophole for $1 < \tan\beta < 1.02$ and small $m_{1/2}, -\mu$ appears for large values of m_0 corresponding to $m_{\tilde{\nu}} > m_{\chi^\pm}$. We have checked whether this loophole may be excluded completely by experimental upper limits on W^\pm decays into charginos and neutralinos. This is not the case with the present limit of 109 MeV on possible non-standard contributions to the W^\pm width, but might be the case in the future, when improved upper limits from LEP and the Tevatron become available. However, this small region could be excluded completely by a small increase in the integrated luminosity available for this analysis, as could probably be obtained by combining the data available to the four LEP experiments (see also [6]). Therefore, we believe that this small loophole is actually illusory, though it is also excluded by the theoretical considerations we discuss later.

3 Cosmological Constraints

Since one of our principal interests in this paper is supersymmetric dark matter, we next apply the cosmological constraint that the relic χ density not be too large, and preferably in the range favoured by theories of structure formation based on inflation, which predicts a total mass density $\Omega \simeq 1$. Models with mixed hot and cold dark matter and a flat spectrum of primordial perturbations, with a cosmological constant and cold dark matter, and with cold dark matter and a tilted perturbation spectrum, all favour the range [19]

$$\Omega_{\text{CDM}}h^2 = 0.2 \pm 0.1 \tag{6}$$

We have computed $\Omega_\chi h^2$ in the (M_2, μ) domain of interest [18], varying m_0 to obtain a result in the above range (6).

The contours of $m_{\tilde{\nu}}$ required to obtain the central value $\Omega_\chi h^2 = 0.2$ for negative μ are displayed in Fig. 2. *We see that the effect of the cosmological constraint (6) is, qualitatively, to constrain the value of $m_{\tilde{\nu}}$, so that it is generally large and bounded away from the dangerous loophole region.* Figs. 2(b,c,d) are complicated by the presence of Z^0 and Higgs poles: near $m_\chi \approx m_Z/2$ and $m_\chi \approx m_h/2$, the neutralino relic density can vary rapidly with m_χ , as annihilation through Z^0 and Higgs bosons via the Higgsino component of the neutralino becomes enhanced. The correct treatment of this enhancement requires calculational techniques beyond the usual non-relativistic expansion in powers of the annihilating relic velocity [7], as discussed in [20]. In Figs. 2(b,c,d), we label by ‘Z’ two contours, connected by a hatched region, corresponding to the vicinity of the Z^0 pole: Ω_χ first falls below 0.2 as the Z^0 pole is approached, and then rises back through 0.2 as the pole is left behind. Similarly, there are two contours labelled ‘H’ in Figs. 2(a,b,c). In Fig. 2(d), the Higgs and Z^0

poles for $m_{\tilde{\nu}} = 150$ GeV and $m_{\tilde{\nu}} = 200$ GeV lie close enough together that Ω_χ remains less than 0.2 for all m_χ between $m_h/2$ and $m_Z/2$. In Fig. 2(a), there is no comparable Z^0 pole structure, since for this value of $\tan\beta$ the Higgsino component of the neutralino is too small to provide significant annihilation through Z^0 bosons. The positions of the Z^0 and Higgs pole contours are roughly independent of $m_{\tilde{\nu}}$ for large values of $|\mu|$. However, there are no Higgs or Z^0 pole contours for $m_{\tilde{\nu}} \lesssim 100$ GeV, as in this case Ω_χ is already less than 0.2 away from the poles. Lastly, we note that stop mixing becomes significant for large $|\mu|$ and one of the \tilde{t} may become tachyonic when $m_{1/2}$ is small. This is the reason why the $m_{\tilde{\nu}} = 100$ GeV contours do not extend to $\mu = -400$ GeV in Figs. 2(a) and 2(b). However, if one adjusts the trilinear soft supersymmetry-breaking parameter A_t , these contours could be extended to $\mu = -400$ GeV without affecting the positions of the non-pole and Z^0 -pole contours.

The implications of this relic-density analysis are carried over to Fig. 3, where we show the $(m_{1/2}, m_0)$ parameter region which admits neutralino relic densities in the cosmologically-favored range given by (6). The area below the light-shaded region leads to relic densities $\Omega_\chi h^2$ which are less than 0.1 for any value of $\mu < 0$. In the light-shaded region, by making $|\mu|$ small (but allowed) one can produce a large Higgsino component for the neutralino, which can then annihilate readily through Z^0 and Higgs bosons. This enables $\Omega_\chi h^2$ to stay below 0.3, whatever the value of m_0 . For this reason, the light-shaded region extends all the way to the top of Fig. 3. Most of the band allowed by cosmology lies above the ALEPH lower limit on $m_{1/2}$ [6], but the tail of it crosses the ‘dangerous’ region where $m_{\chi^\pm} > m_{\tilde{\nu}}$. However, we see in Fig. 3 that the cosmologically-allowed part of this ‘dangerous’ region is largely excluded by other phenomenological constraints, in particular by the single-photon experiments [10]. The residual part of this ‘dangerous’ region may be excluded by certain additional model assumptions, as we discuss below.

4 Electroweak Symmetry Breaking Constraints

Further constraints on the MSSM parameters can be obtained from other, more theoretical, considerations. In particular, it is attractive to believe that electroweak symmetry breaking (EWSB) is driven by radiative corrections to soft supersymmetry-breaking Higgs masses in the MSSM [11]. Quantifying this constraint requires additional assumptions beyond the normal renormalization group running of the MSSM parameters, notably the assumption that the Higgs masses are equal to the other scalar masses m_0 at the supersymmetric grand unification scale. Making this universality assumption, *one obtains a definite value of μ* , for any given values of the other MSSM parameters $(m_0, m_{1/2}, A, \tan\beta)$ [21]. This is displayed

in the right-hand side of Fig. 2 for m_0 varied over the interesting range, for a minimum value of the top mass: $m_{\text{top}} = 161$ GeV. The constraint for $\mu < 0$ is identical.

The application of the EWSB constraint on μ strengthens the ALEPH lower bound on m_χ . When μ is fixed in this way, as seen in Fig. 2, the LSP is predominantly gaugino, and the annihilation proceeds through sfermion exchange and hence is sensitive to m_0 . The dark-shaded regions in Figs. 3(b,c) delimit the cosmologically-favored zones in the case $\mu < 0$: the effect of the Higgs pole [20] is evident for $m_{1/2} \simeq (40, 65)$ GeV, and the bottom side of the Z^0 pole appears when $m_{1/2} \gtrsim 90$ GeV. The difference from the light-shaded region, which does not exhibit such any indentations, appears because EWSB forbids one from varying μ freely in the manner described in the previous section. The dark regions are cut off at low $m_{1/2}$ by the absence of radiative EWSB solutions for the values of $m_{\text{top}} \geq 161$ GeV which we assume: larger values of m_{top} would permit EWSB only in a smaller domain of parameter space. The bounds derived from the chargino and neutralino searches become more stringent when μ is fixed by EWSB, as indicated by the solid lines in Figs. 3(b,c,d) (marked ‘EWSB’). The combination of EWSB and cosmology shown in Fig. 3(b) still allows, apparently, a tiny subset of the ‘dangerous’ region at small $m_{1/2}$ and $m_0 \simeq 60$ GeV. However, this subset is in fact excluded by the LEP lower limit on the mass of the lighter neutral scalar Higgs boson in the MSSM [22], as also discussed in [6]. The bounds from neutralinos cover the ‘dangerous’ chargino region when $\tan\beta = 2$, as can be seen in Fig. 3(c). For the case of $\tan\beta = 1.01$ shown in Fig. 3(a), we find no experimentally consistent EWSB solution, as discussed in more detail below. In the case of $\tan\beta = 35$ shown in Fig. 3(d), EWSB implies an LSP which has a large Higgsino admixture, and whose relic density is less than 0.1 independent of m_0 in the range of $m_{1/2}$ plotted, so there is no dark-shaded region in Fig. 3(d). We exhibit in Figs. 3(b,d) how the lower limit on the chargino mass is recovered when $m_{\tilde{\nu}} \lesssim m_{\chi^\pm} - 3$ GeV, once the value of μ is fixed by the EWSB constraint.

5 Lower Bounds on the Neutralino Mass

As seen in Fig. 3, for $\mu < 0$ and different values of $\tan\beta$, one obtains a series of lower bounds on the neutralino mass, depending on the assumptions applied. We exemplify these for the case $\tan\beta = \sqrt{2}$, for which LEP 1 alone provided no rigorous lower bound on m_χ , whilst the purely experimental bound from the combination of LEP 1 and 1.5 is less sensitive than for larger $\tan\beta$:

- The ALEPH experimental bound for large m_0 , which is not a notably conservative assumption, in view of the loopholes discussed above: $m_\chi \gtrsim 17$ GeV;

- Combination of the ALEPH experimental bound for arbitrary m_0 with the limits from other unsuccessful sparticle searches, notably the AMY bound [10], which eliminates the possibility that $M_2 = 0$: $m_\chi \gtrsim 5$ GeV;
- Combining the above experimental limits with the cosmological constraint on $\Omega_\chi h^2$, which has the effect of favouring large values of m_0 , and disregarding the residual loop-hole region where $m_{\chi^\pm} \gtrsim m_{\tilde{\nu}}$: $m_\chi \gtrsim 16$ GeV, representing a significant improvement on the purely experimental bound in the previous case;
- Combining the experimental constraints with both the cosmological constraint on $\Omega_\chi h^2$ and the assumption of dynamical EWSB³, which improves further on the bound in the previous case: $m_\chi \gtrsim 24$ GeV.

Before discussing the dependence of these various lower bounds on $\tan\beta$, we first note that dynamical EWSB is possible in the range of parameters studied only if $\tan\beta$ is sufficiently large. If $\tan\beta$ is too small, either the top quark mass $m_{\text{top}} \lesssim 160$ GeV, in conflict with the Tevatron measurements [23], or the running of the top-quark Yukawa coupling becomes non-perturbative at large scales. Even if one believes the perturbative renormalization-group equations in this case, we find that the lighter stop squark mass $m_{\tilde{t}}$ now falls below the absolute lower limit from LEP. We find the restriction

$$\tan\beta \gtrsim 1.2, \tag{7}$$

which is shown as the vertical wavy line in Fig. 1. This has the effect of strengthening somewhat the lower limit on m_χ , and also closes independently the small $M_2, |\mu|$ loophole for $\tan\beta \leq 1.02$, which, as we mentioned earlier, could also presumably be excluded by combining the data of all the LEP collaborations.

We now return to Fig. 1, which displays as functions of $\tan\beta$ our new limits on the neutralino mass for $\mu < 0$, compared with the direct ALEPH experimental lower bound [6] for large $m_{\tilde{\nu}}$, shown as a dashed line. The dotted line is the more conservative experimental lower bound, obtained by allowing $m_{\tilde{\nu}}$ to vary freely, but taking other sparticle searches into account. The dash-dotted line is obtained by imposing the cosmological constraint on $\Omega_\chi h^2$, and ignoring the residual loophole region. Finally, the solid line is obtained by combining all experimental, cosmological and EWSB constraints.

The irregularities in this line are related to the Higgs and Z^0 pole effects on $\Omega_\chi h^2$, and are best illustrated by referring to Figs. 3(b,c). We see in Fig. 3(b) that, when $\tan\beta$ is in

³We note that applying the EWSB constraint by itself does not improve significantly the purely experimental lower bound on m_χ , unless the indirect constraint from the MSSM Higgs search is used.

a range around $\sqrt{2}$, the lower bound on $m_{1/2}$ and hence m_χ is given by the intersection of the EWSB line with the central ‘island’ of the dark-shaded cosmological region, between the Higgs and Z^0 poles. As $\tan\beta$ is increased, the Higgs pole region moves to the right, eroding the central ‘island’, until the EWSB line starts missing it altogether and passes along the ‘channel’ between the ‘island’ and the left-hand dark-shaded region. This occurs for $\tan\beta \simeq 1.7$, so the lowest allowed value of m_χ is then given by the extreme left end of the ‘island’ until the EWSB line starts hitting the left-hand dark-shaded region, which occurs when $\tan\beta \simeq 2$, as seen in Fig. 3(c). Thereafter, the lower limit on m_χ is provided by the intersection of the EWSB line with this left-hand region. This is the reason why the dependence of the lower limit on $\tan\beta$ is different in the regions $\tan\beta = 1.2 - 1.7$, $1.7 - 2$ and above 2, as seen in Fig. 1⁴. As $\tan\beta$ is increased further, eventually the Higgs and Z^0 pole ‘channels’ coalesce, and the central ‘island’ disappears. The contact between the EWSB line and the left-hand dark-shaded region is lost when $\tan\beta$ reaches ≈ 5 , after which the lower limit on m_χ is given by the left-hand point of the right-hand dark-shaded region. This is the reason for the jump in the bound at $\tan\beta \approx 5$.

We obtain from the solid line in Fig. 1 the following absolute lower bound on the neutralino mass for $\mu < 0$:

$$m_\chi \geq 21.4 \text{ GeV} \quad (8)$$

As already mentioned, we do not discuss the case $\mu > 0$ in great detail in this paper, deferring a complete discussion to a subsequent paper. The ALEPH analysis does not have the same sort of loophole at large m_0 as in the case $\mu < 0$, and the behavior for smaller m_0 is not as complex as for $\mu < 0$. A conservative lower limit $m_\chi \gtrsim 26 \text{ GeV}$ is provided by the LEP 1 lower limit of 45.5 GeV on the chargino mass, which remains valid even when $m_{\chi^\pm} \gtrsim m_{\tilde{\nu}}$. When $\tan\beta \gtrsim 3$, cosmology and EWSB strengthen this limit considerably, since $m_{1/2}$ must be to the right of a pole-induced ‘channel’ analogous to those shown in Figs. 3(b,c), and we find that $m_\chi \gtrsim 56 \text{ GeV}$, for large $m_{\tilde{\nu}}$. For $\tan\beta \lesssim 3$, the limit is somewhat weaker: $m_\chi \gtrsim 36 \text{ GeV}$, again for large $m_{\tilde{\nu}}$.

Assuming gaugino mass universality, our lower limit (8) on m_χ can be compared with the D0 lower limit [24] on the gluino mass. The D0 collaboration excludes gluino masses below 175 GeV for all squark masses, with little sensitivity to μ and $\tan\beta$, and imposes a lower limit of 220 GeV on degenerate gluino and squark masses. This D0 constraint may

⁴The lower bound on m_χ may be further strengthened when $\tan\beta \lesssim 2.5$ by taking into account the LEP 1 limits on the MSSM Higgs mass, as discussed in [6]. The amount by which the bound is strengthened depends somewhat on other MSSM parameters besides those discussed here, and we defer further discussion to a subsequent paper.

be mapped into the $(m_{1/2}, m_0)$ plane using the MSSM mass relations, as indicated by the dotted lines in Fig. 3. It imposes a lower limit on $m_{1/2}$ that depends relatively weakly on m_0 , and is stronger than that of LEP 1 and 1.5 for small values of $\tan\beta$, as may be seen from the horizontal long-dashed line in Fig. 1. However, Fig. 1 shows that stronger limits on m_χ may be obtained from cosmological and/or dynamical EWSB considerations⁵.

6 Conclusions and Prospects

The recent ALEPH experimental analysis [6] has enabled a qualitative step forward to be made in bounding the mass of the lightest neutralino. The LEP 1 and 1.5 data combine to exclude regions of parameter space that could not be excluded by either data set in isolation. However, the ALEPH analysis could not exclude entirely the possibility when $\mu < 0$ that $m_{1/2} = 0$, and hence $m_\chi = 0$. We have shown in this paper that this loophole may be excluded by other experimental data [10], leading to a lower bound on m_χ that may be strengthened significantly by constraining the relic density $\Omega_\chi h^2$, with further improvement possible if one assumes dynamical EWSB. Combined, these constraints provide a lower limit on m_χ that is stronger even than that inferred indirectly from the unsuccessful gluino search of the D0 collaboration. In the near future, data from higher-energy runs of LEP around and above the W^+W^- threshold (which we call LEP 2W) will be able to explore definitively the loopholes in the recent ALEPH experimental analysis, making the theoretical appeal to cosmology and EWSB unnecessary.

Although we do not wish to prejudge the results of these future searches, it already seems likely that the neutralino mass must be considerably larger than previous experimental limits, with strong implications for some dark matter search experiments. Some of these are optimized for $m_\chi \lesssim 10$ GeV [8], whilst all direct search experiments may benefit from the higher nuclear recoil energies now to be expected. On the other hand, rates for both direct and indirect dark matter searches are generally reduced as m_χ increases. Thus, the recent LEP 1.5 run and future LEP 2W data at higher energies may have significant impact on the search for supersymmetric dark matter.

⁵We emphasize that the D0 constraint shown in Figs. 1, 3 holds only if one imposes equality between the gluino and electroweak gaugino masses at the GUT scale. It is clear from Fig. 3 that the purely experimental LEP 1.5 constraint on $m_{1/2}$ at small $\tan\beta$ could also become stronger than the limit inferred from D0 if the GUT relation were violated by a factor of two or so. However, an exploration of non-universality in the gaugino masses lies beyond the scope of this paper.

Acknowledgments

J.E. would like to thank the University of Minnesota, Lawrence Berkeley National Laboratory and the Berkeley Center for Particle Astrophysics for kind hospitality while parts of this work were being done. M.S. would like to thank Jean-Francois Grivaz and Laurent Dufлот for valuable discussions. This work was supported in part by DOE grant DE-FG02-94ER-40823.

References

- [1] ALEPH Collaboration, D. Buskulic et al., Phys. Lett. **B373** (1996) 246.
- [2] OPAL Collaboration, G. Alexander et al., CERN preprint PPE/96-20 (1996).
- [3] L3 Collaboration, M. Acciarri et al., CERN preprint PPE/96-29 (1996).
- [4] DELPHI Collaboration, P. Abreu et al., CERN preprint PPE/96-75 (1996).
- [5] For reviews, see: H.P. Nilles, Phys. Rep. **110** (1984) 1; H.E. Haber and G.L. Kane, Phys. Rep. **117** (1995) 75.
- [6] ALEPH Collaboration, D. Buskulic et al., CERN-PPE/96-83 (submitted to Zeitschrift für Physik).
- [7] J. Ellis, J.S. Hagelin, D.V. Nanopoulos, K.A. Olive and M. Srednicki, Nucl. Phys. **B238** (1984) 453.
- [8] C. Absmeier et al., Max-Planck-Institut, München preprint MPI-PHE-95-15 (1995); see also A. Gabutti et al., hep-ph/9602432.
- [9] see J.R. Primack, D. Seckel, B. Sadoulet, Ann. Rev. Nucl. Part. Sci. **38** (1988) 751, and references therein.
- [10] AMY Collaboration, Y. Sugimoto et al., Phys. Lett. **B369** (1996) 86.
- [11] L.E. Ibanez and G.G. Ross, Phys. Lett. **B110** (1982) 215; L.E. Ibanez, Phys. Lett. **B118** (1982) 73; J. Ellis, D.V. Nanopoulos and K. Tamvakis, Phys. Lett. **B121** (1983) 123; L. Alvarez-Gaumé, J. Polchinski and M.B. Wise, Nucl. Phys. **B221** (1983) 495; K. Inoue, A. Kakuto, H. Komatsu and S. Takeshita, Prog. Th. Phys. **68** (1982) 927.
- [12] ALEPH Collaboration, D. Buskulic et al., Phys. Rep. **216** (1992) 253.

- [13] Particle Data Group, Phys. Rev. **D50** (1994) 1173.
- [14] The LEP Collaborations ALEPH, DELPHI, L3, OPAL and the LEP Electroweak Working Group, CERN preprint PPE/95-172 (1995).
- [15] P. Fayet, Phys. Lett. **B69** (1977) 489.
- [16] J. Ellis and J.S. Hagelin, Phys. Lett. **B122** (1983) 303.
- [17] K. Grassie and P.N. Pandita, Phys. Rev. **D30** (1984) 22.
- [18] J. McDonald, K.A. Olive, and M. Srednicki, Phys. Lett. **B283** (1992) 80.
- [19] For a review and references, see V. Berezinsky et al., CERN preprint TH/96-42, hep-ph/9603342.
- [20] K. Griest and D. Seckel, Phys. Rev. **D43** (1991) 3191; P. Gondolo and G. Gelmini, Nucl. Phys. **B360** (1991) 145.
- [21] For a review and references, see J. Ellis, Rapporteur Talk at the International Symposium on Lepton and Photon Interactions at High Energies, Beijing 1995, CERN preprint TH/95-316, hep-ph/9512335.
- [22] ALEPH Collaboration, D. Buskulic et al., *Search for the $hA \rightarrow b\bar{b}b\bar{b}$ final state in two Higgs doublet models*, contributed paper EPS0415 to the International Europhysics Conference on High Energy Physics, Brussels 1995.
- [23] CDF Collaboration, F. Abe et al., Phys. Rev. Lett. **74** (1995) 2676; D0 Collaboration, S. Abachi et al., Phys. Rev. **74** (1995) 2632.
- [24] D0 Collaboration, S. Abachi et al., *Search for Squarks and Gluinos in $p\bar{p}$ Collisions at the D0 Detector*, contributed paper No. 434 to the Int. Europhys. Conf. on High Energy Physics, Brussels, 1995.

Figure Captions

Fig. 1) The ALEPH lower limit on m_χ [6] for $\mu < 0$ and for large $m_{\tilde{\nu}}$ (short-dashed line) is compared, as a function of $\tan\beta$, with the results obtained in the text by making different phenomenological and theoretical inputs. The dotted line is obtained by combining the AMY constraint [10] with other unsuccessful searches for sleptons and sneutrinos: it excludes the region of $\tan\beta$, indicated by a double arrow, where the ALEPH experimental limit does not exclude $m_\chi = 0$. The dash-dotted line is obtained by requiring also that the cosmological relic neutralino density fall within the preferred range (6). The solid line is obtained by combining these experimental and cosmological inputs with the assumption [11] of dynamical electroweak symmetry breaking. The vertical wavy line indicates the lower limit on $\tan\beta$ in such dynamical electroweak symmetry breaking models. The horizontal long-dashed line is that obtained from the D0 gluino search [24], assuming gaugino mass universality.

Fig. 2) The region of the (μ, M_2) plane excluded by direct searches [1] for (A) charginos at LEP 1.5, (B) neutralinos at LEP 1.5 and (C) Z^0 decays into $\chi\chi'$ at LEP 1 for $\tan\beta = 1.01, \sqrt{2}, 2, 35$ are indicated in (a,b,c,d) respectively by thin solid lines. Contours of $m_{\tilde{\nu}}$ (in GeV) required in the MSSM to obtain $\Omega_\chi h^2 = 0.2$ for $\mu < 0$ are indicated by thick solid lines. The hatched regions indicate where the Higgs and Z^0 poles suppress the relic density, as discussed in the text. Values of μ required by dynamical electroweak symmetry breaking for the indicated values of m_0 (in GeV) are shown as short-dashed lines in (b,c,d) for $\mu > 0$: identical values would be required for $\mu < 0$.

Fig. 3) For $\tan\beta = 1.01$ (a), $\sqrt{2}$ (b), 2 (c) and 35 (d), we display for $\mu < 0$ the domains of the $(m_{1/2}, m_0)$ plane that are excluded by the ALEPH chargino and neutralino searches [6] (long-dashed line), by the limit (3) on $m_{\tilde{\nu}}$ (short-dashed line), by the LEP limits [1, 3] on slepton production (solid line), by single-photon measurements [10] (grey line), and by the D0 limit on the gluino mass [24] (dotted line). The region of the plane in which $0.1 < \Omega_\chi h^2 < 0.3$ for some experimentally-allowed value of $\mu < 0$ is light-shaded, and the region of the plane in which $0.1 < \Omega_\chi h^2 < 0.3$ for μ determined by dynamical electroweak symmetry breaking is shown dark-shaded in (b,c). The constraint derived from the ALEPH searches when imposing dynamical electroweak symmetry breaking (EWSB) is also shown as a solid line in (b,c,d).

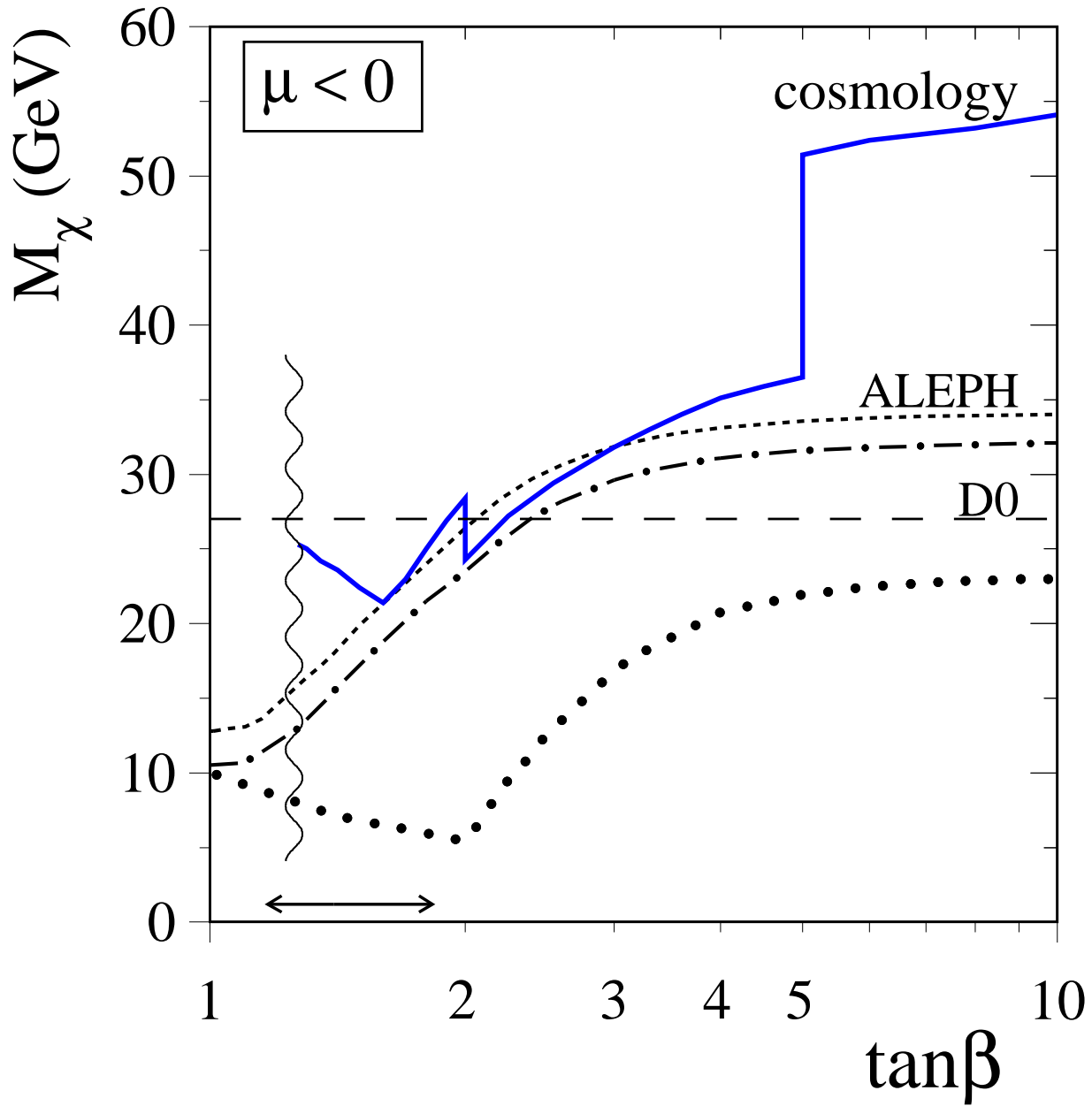


Figure 1:

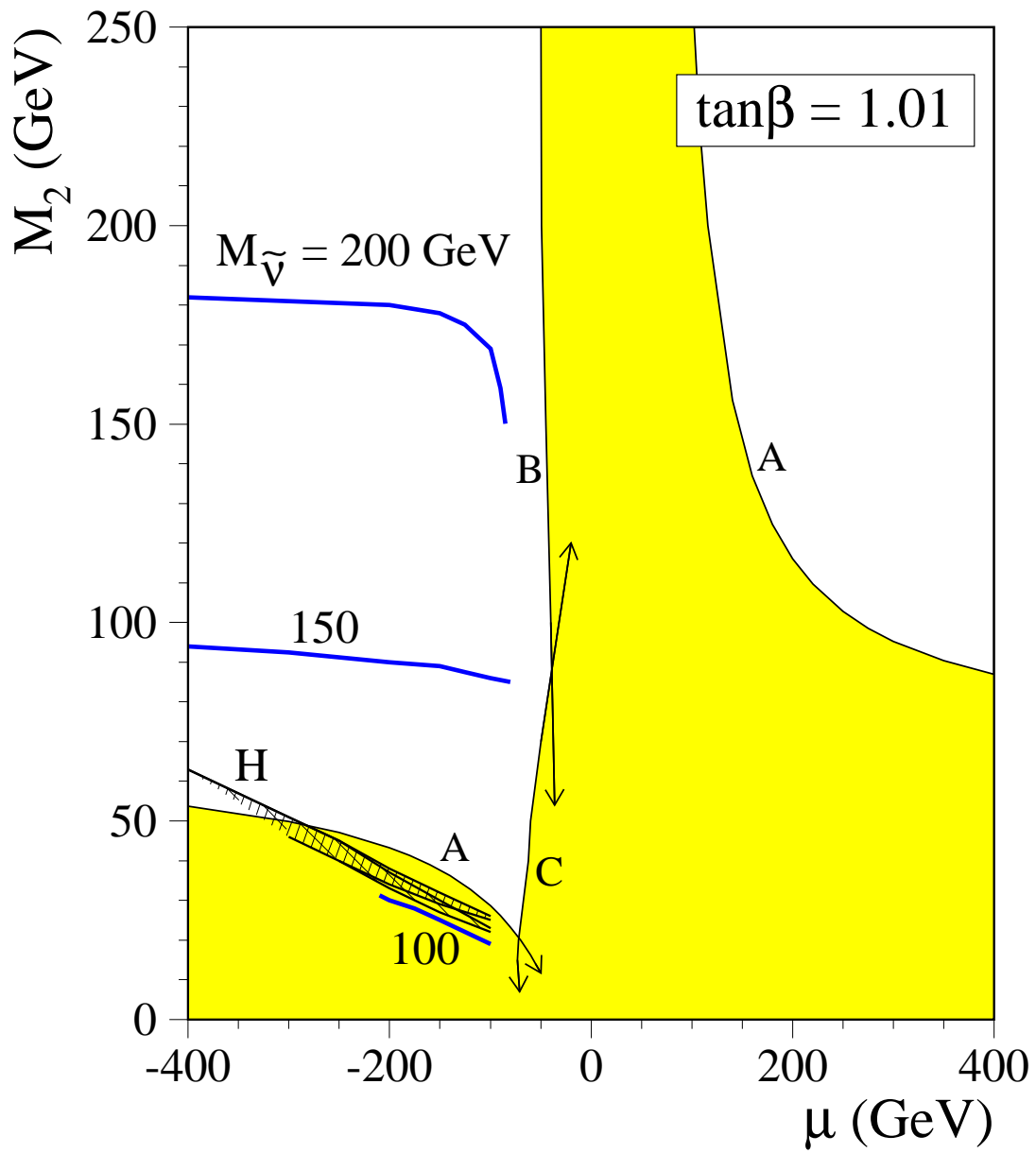


Figure 2: a

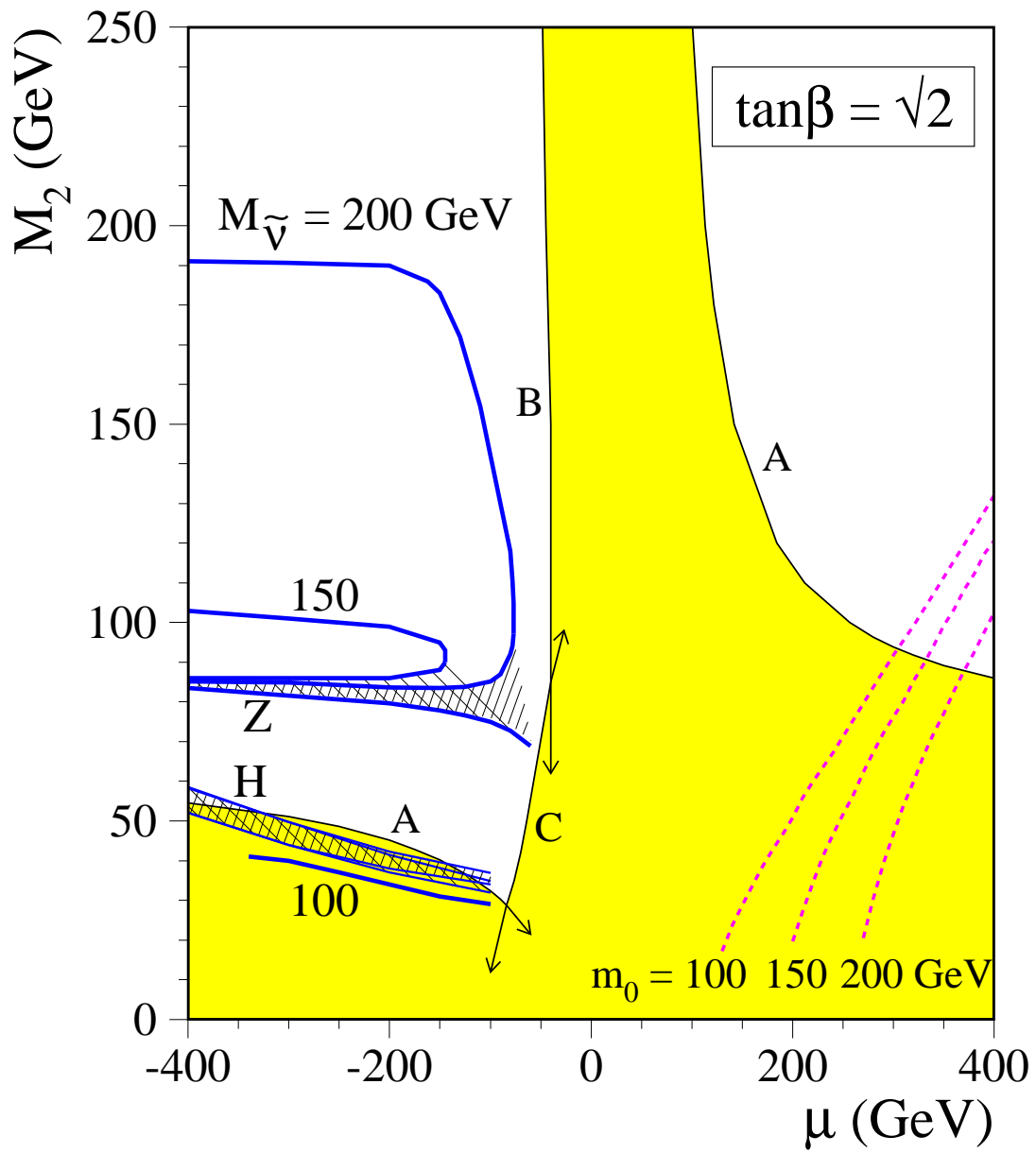


Figure 2: b

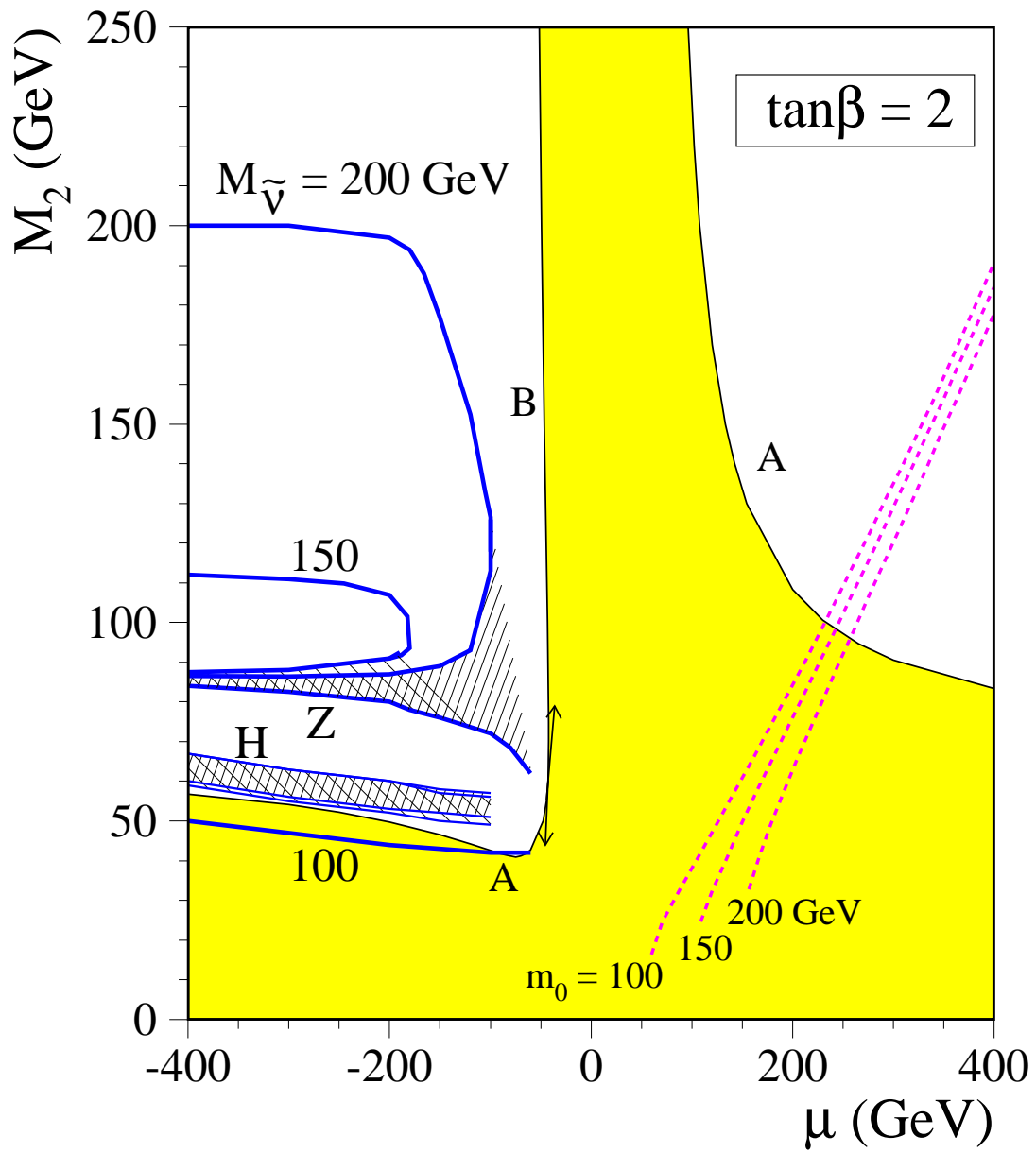


Figure 2: c

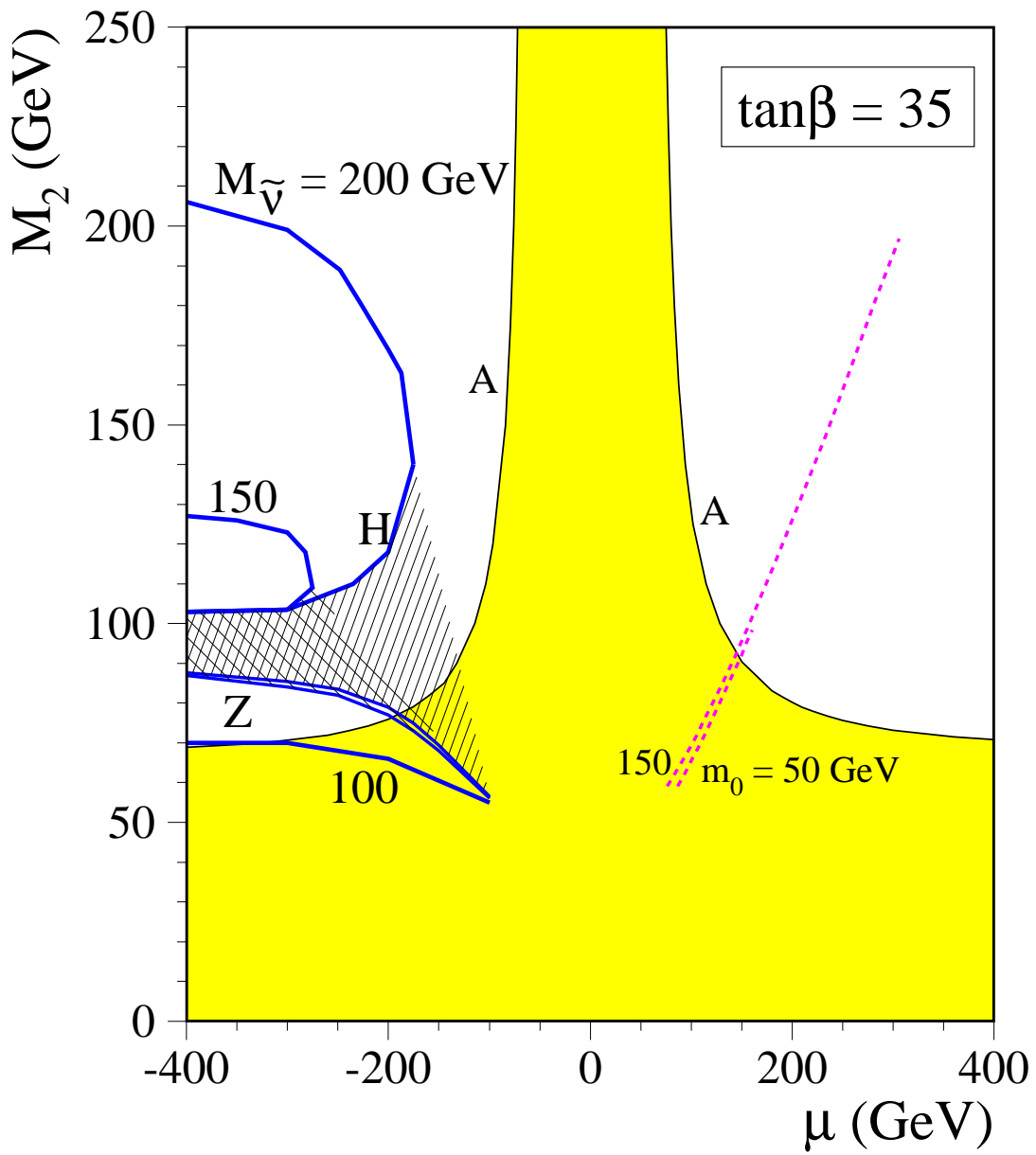


Figure 2: d

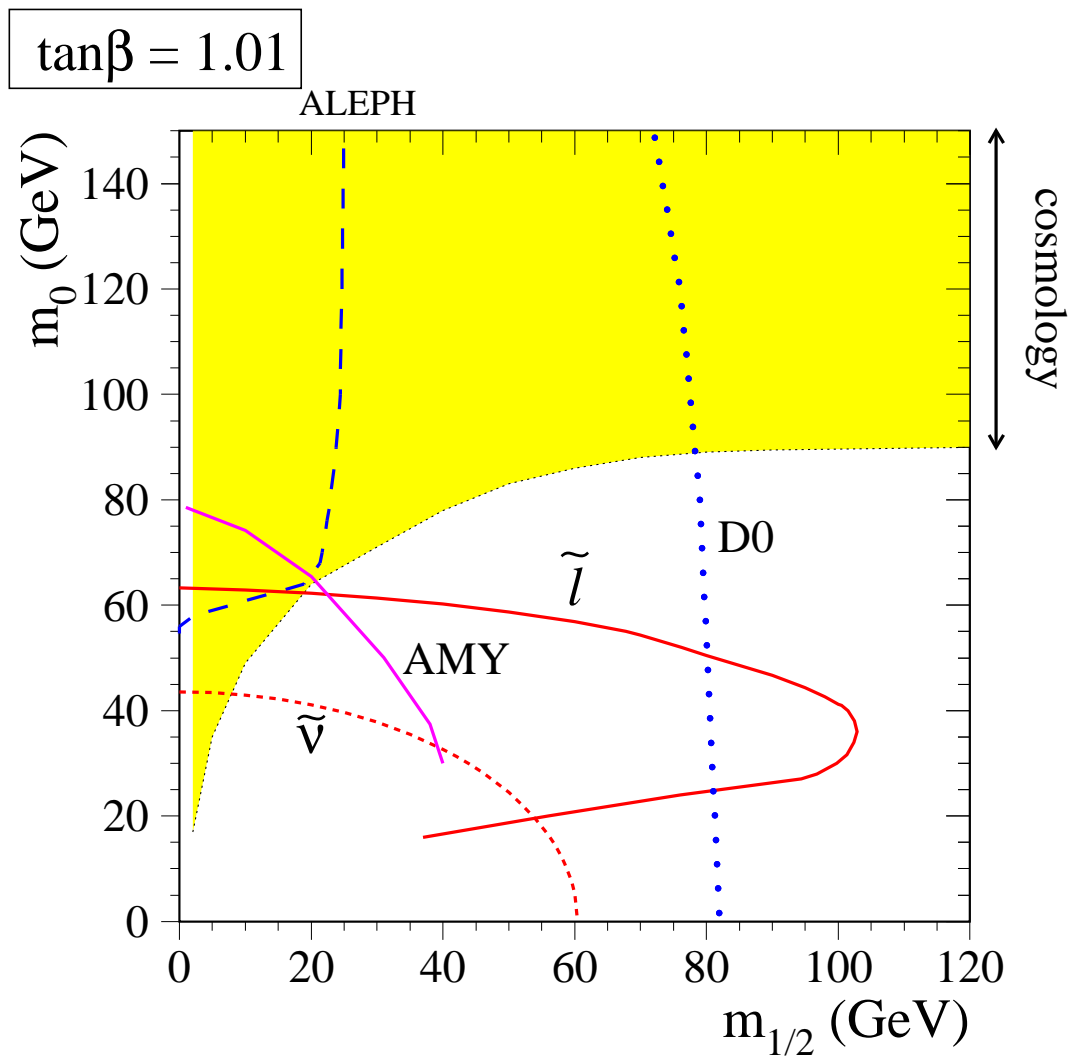


Figure 3: a

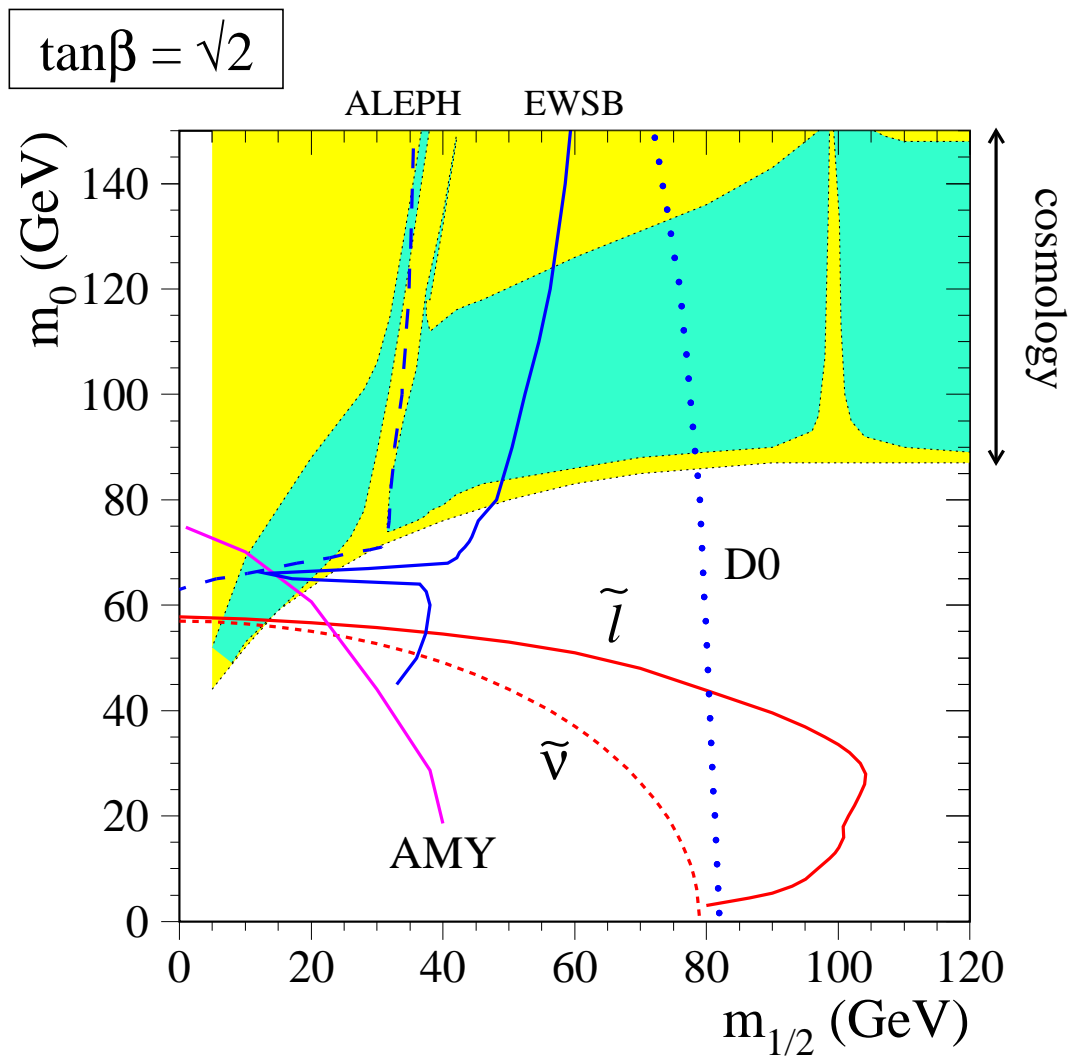


Figure 3: b

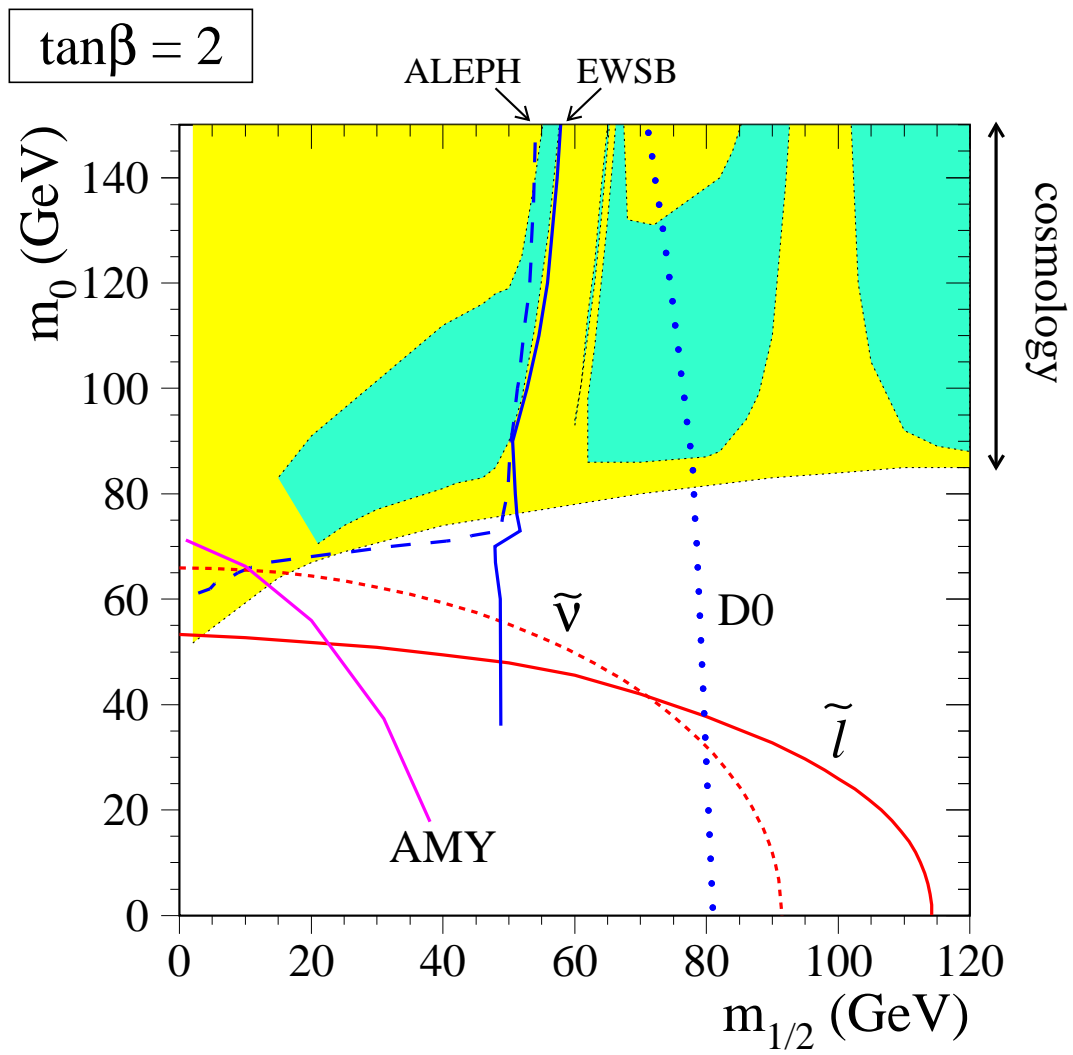


Figure 3: c

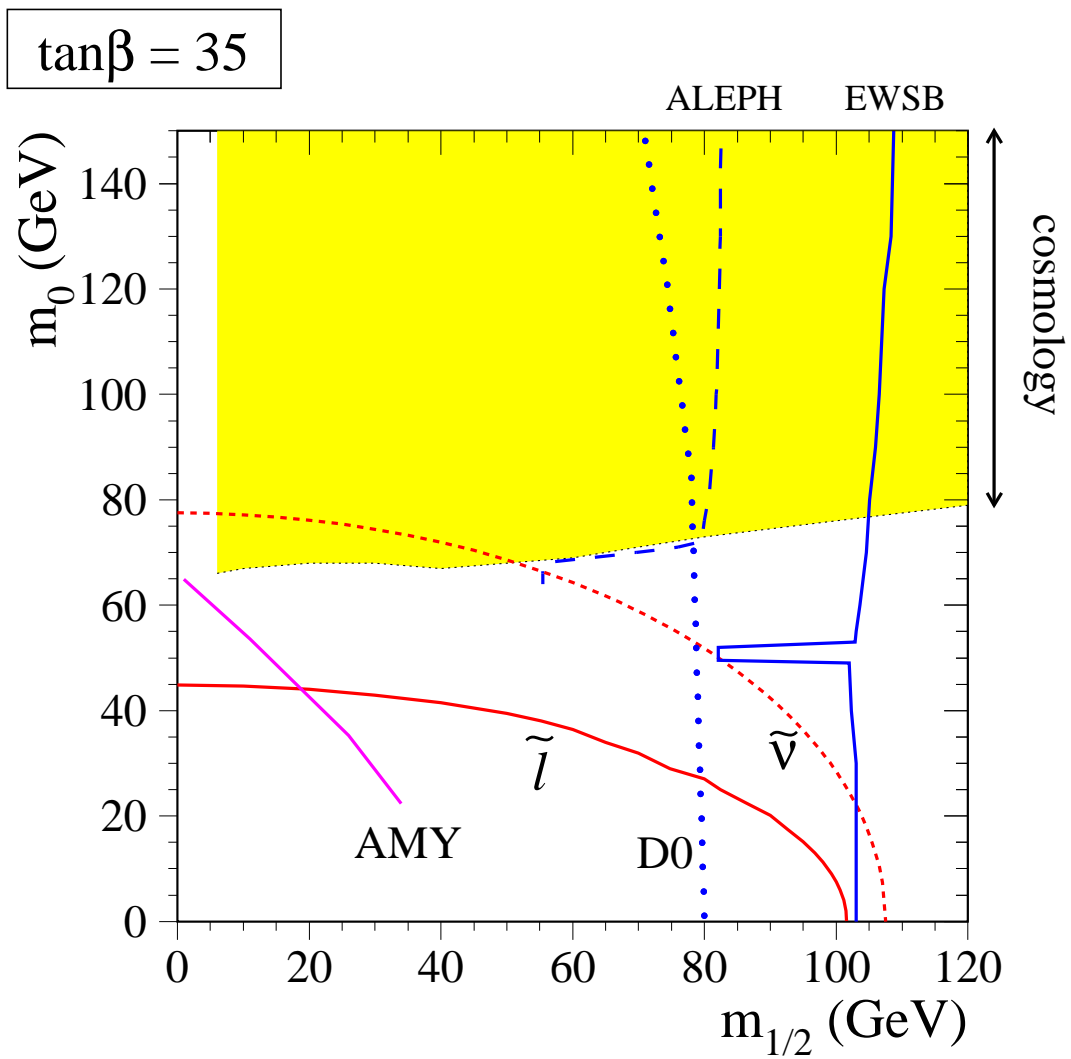


Figure 3: d